Compositional variations of olivine in shonkinite and its associated ultrabasic rock from the carbonatite complex of Tiruppattur, Tamil Nadu

R. Ramasamy*, S. P. Subramanian and R. Sundaravadivelu

Department of Ocean Engineering,
Indian Institute of Technology–Madras, Chennai 600 036, India

The compositional variations of olivine from shonkinite (shon) and associated ultrabasic rock (ubr) are analysed and an attempt is made to trace their magmatic evolution. The analysed olivine in shon is subjected to a prolonged period of magmatic crystallization with the development of zoning of augite, aegirine-augite and jadeite at its peripheral portions by reaction with residual magma. On the other hand, the composition of olivine from ubr represents intermediate position in the course of magmatic evolution of olivine occurring in shon. The high concentration of Ca–Na–K–Al in olivine from ubr indicates its kimberlitic affinity. These features indicate that shon magma is the parent magma for ubr. The shon occurs in the form of nodules/xenoliths in ubr, which is a member of the ultrabasic complex in this area. Further study is required to isolate ubr of kimberlitic affinities from the ultrabasic complex enclosing the potash-rich alkali syenites at the inner portion of Jogipatti basin, which is a part of the Tiruppattur carbonatite complex, Tamil Nadu.

Keywords: Carbonatite complex, kimberlite, olivine, shonkinite, ultrabasic rock.

THE Tiruppattur carbonatite complex (12°00′00″–12°30′00″N and 78°25′00″–78°35′00″E), Tamil Nadu, India, is emplaced in two adjacent structural basins separated by E–W and NW–SE trending faults. The northern basin called Sevvattur basin is enclosed with ultrabasic rocks (ubrs), comprised of sequences of the co-magmatic series of soda-rich alkali syenites and carbonatites towards the inner portions. The co-magmatic activity had shifted and continued in the southern Jogipatti basin, which uplifted and rotated during this period. The magmatic activity caused emplacement of sequences of the co-magmatic series of potash-rich syenites within an ultrabasic complex enclosing the Jogipatti structural basin[1,2]. Shonkinite (shon) occurs (12°16′08″N, 78°28′26″E) in the Jogipatti basin near Kanjanur Village at the foot of a hillock (12°16′22″N, 78°28′28″E) of an ubr subjected to stock-works of magnesite. Though shon was exposed as a very large body of dyke-like rocks more than 40 years ago at this place[1,3], it was completely removed as building stone and no exposure is found at present at the foothills of ubr. Now it is exposed in the southern portion of the ultrabasic hillock only in well sections as nodules and xenoliths (12°16′08″N, 78°28′26″E). The ubr is one of the members of the ultrabasic complex which is composed of several sheets, nodules, xenoliths and dykes of dunites, peridotites, pyroxenites, sulphide-bearing pyroxene–biotite–amphibolite, vermiculite-bearing peridotite, stock-works of magnesite, carbonatite (including benstonitic, ankeritic, sovitic and beforsitic) and veinlets of barite, apatite–magnetite–ilmenorutile, riebeckite–monazite–albitite and riebeckite–calcite schists. The ultrabasic complex encloses a series of co-magmatic potash-rich alkali syenites and carbonatites in the inner portion of the basin.

The shon from the carbonatite complex of Tiruppattur[1–4] is composed of equal proportions of glistening grains of euhedral minerals of clinopyroxenes (cpx) and potash feldspars (predominantly of anorthoclase or sanidine in composition) with essential accessories of olivine (ol), hornblende, biotite, apatite and magnetite. The rock exhibits pandiomorphic texture with intersertal grains of lath-shaped potash feldspars. Detailed petrographic geochemical studies of ol, augite, hornblende and biotite from shon reveal co-existence of both early-formed and late-formed mafic minerals together in this rock[3,4]. It is also suggested that shon is the intermediate in bulk-rock chemical composition between the ubrs occurring in this complex and the alkali syenites varying from the sodic and potassic series[2,4]. It has been reported that shon magma is the parent magma for both ubrs and associated alkali syenites and carbonatites[3].

The ultrabasic complex in this area is comprised of members of wide compositional variations, ranging from lamproite, kimberlite, dunite, peridotite and pyroxenite. In this communication, an attempt has been made to study the geochemical variation of an ol grain in shon with six spot analyses of the single grain. The geochemistry of ol from shon is correlated with five spot analyses of ol from an ubr associated with shon. The ubr associated with shon is essentially composed of volume proportions of ol 35%, augite 40%, hornblende 10%, phlogopite 7%, andesine 5%, magnetite 2% and ilmenite 1%. The ubr represents the composition of a peridotite. Under thin-section examination, the rock exhibits fine-grained granular texture. The peripheral portions of ol and cpx are colourless to pale green in nature and they exhibit low interference first-order grey colour, indicating development of jadeite. The detailed petrography and geochemistry of shon has already been described[3]. Grains showing typical euhedral ol forms and cracks are selected in these rocks and are examined under high resolution scanning electron microscope (SEM) attached with Energy Dispersive X-ray micro-Analysis (EDAX) probe to study the geochemical variations (Figure 1).

*For correspondence. (e-mail: drrramy@ymail.com)

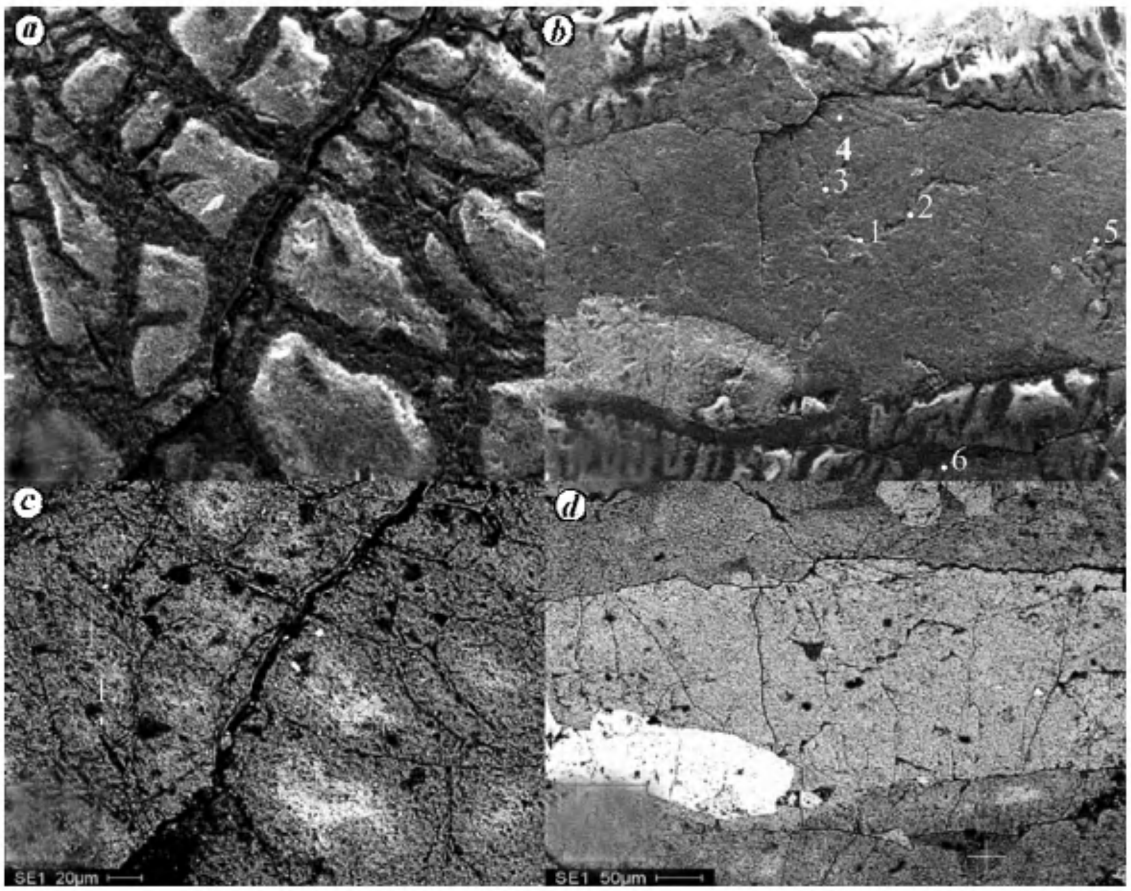

Figure 1. Electron photomicrographs of olivine in shonkinite (shon) from Kanjanur, Tiruppattur complex. ***a***, Olivine crystals showing irregular embayment at X200; ***b***, Polished olivine grain at X100 BSE, showing the site of EDAX analyses; ***c***, EDAX analysis at the core of olivine grain; ***d***, EDAX analysis at the periphery of olivine grain.

The analyses were carried out using Micronsperpixy-0031 attached with an EDAX probe high-resolution SEM in the Metallurgical Laboratory, Indian Institute of Technology, Madras (IITM), Chennai. Initially a thin section was prepared and examined under polarizing microscope to select a suitable grain for EDAX analyses. Mineral phases were identified by back-scattered images. Six EDAX micro-spot analyses in an ol grain occurring in shon and five EDAX micro-spot analyses in an ol grain from ubr were carried out from the core to the peripheral portions.

Table 1 indicates that the chemical compositions of peripheral portions of the two ol grains are intermediate in composition between ol and cpx. All these analyses exhibit high concentration of Cr and Ni with characteristic enrichment of Ce, Ba, Sr and S of rocks of the carbonatite complex. The Rittmann's normative calculations[5] indicate that the core portion of the grain analysed in shon or ubr represents the chemical composition of ol. The ol structural formula calculated on the basis of 4(O), indicates that the tetrahedral site is significantly enriched with Si^{iv} ions, except the core portion of the grain in shon. Forsterite and fayalite mol% decrease steadily towards the peripheral portions, but they increase in the ol grain of ubr. Monticellite and kirschsteinite increase in the periphery of ol grain in shon, whereas their variations are not significant in the peripheral portion of the ol grain in ubr. The ol components of NaKAl-orthosilicates increase rapidly towards the peripheral portion of the grain in shon. On the other hand, this component exhibits limited variation, around 30%, in ol analysed in ubr. This feature reveals that ubr possesses kimberlitic affinity[6] by enrichment of Ca–Na–K–Al in the presence of significant mol% of monticellite, kirschsteinite and NaKAl-orthosilicates in their formula units.

The chemical compositions calculated on the basis of 6(O) for cpx indicate that the tetrahedral site is deficient in Si ions and considerable amount of Al^{iii+}, Ti^{iv+}, and Fe^{iii+} ions enter into the tetrahedral lattices. Chemical analyses indicate the presence of ol at the core. Peripheral portions of ol are transformed into augite, aegirine-augite and jadeite. These grains are subjected to oscillatory zoning with the development of zonal rims of different composition at their peripheral portions indicating their magmatic growth. Fe^{iii+} ions are calculated from analysed Fe^{ii+} compositions to meet Si deficiency at the tetrahedral

Table 1. Chemical analysis of olivine in shonkinite and in adjoining ultrabasic rocks

	Shonkinite		Core to periphery			Olivine in ultrabasic rocks			Core to periphery		
Olvine in	1	2	3	4	5	6	7	8	9	10	11
SiO_2	34.52	33.92	49.62	49.34	39.63	42.86	40.74	41.52	43.52	43.21	42.78
Al_2O_3	0.00	0.56	2.96	3.79	8.24	30.73	9.55	10.10	9.82	11.17	10.09
FeO	24.65	23.20	6.53	8.11	5.80	0.44	21.24	20.09	19.49	17.14	19.89
MgO	39.32	34.06	17.85	13.50	12.57	0.55	9.83	9.81	10.74	16.24	10.55
CaO	0.24	1.63	20.25	21.28	19.57	1.68	12.73	11.39	11.16	7.61	10.69
Na_2O	1.02	5.31	1.81	2.97	10.71	16.42	3.04	4.12	2.93	2.83	3.50
K_2O	0.24	1.16	0.37	0.37	2.97	6.87	1.73	1.75	1.52	0.94	1.34
TiO_2	0.00	0.16	0.61	0.65	0.52	0.44	1.14	1.22	0.82	0.86	1.17
Total	100.00	100.00	100.00	100.00	100.00	100.00	100.00	100.00	100.00	100.00	100.00
4 (O)	Olivine structure										
Si	0.959	0.961	1.281	1.289	1.089	1.087	1.128	1.140	1.178	1.141	1.162
Al4+	0.000	0.018	0.000	0.000	0.000	0.000	0.000	0.000	0.000	0.000	0.000
Ti4+	0.000	0.003	0.000	0.000	0.000	0.000	0.000	0.000	0.000	0.000	0.000
Fe3+	0.041	0.018	0.000	0.000	0.000	0.000	0.000	0.000	0.000	0.000	0.000
Al6+	0.000	0.000	0.087	0.112	0.257	0.884	0.300	0.314	0.301	0.335	0.311
Fe	0.510	0.510	0.136	0.170	0.128	0.009	0.473	0.444	0.424	0.364	0.434
Mg	1.567	1.383	0.661	0.506	0.495	0.020	0.390	0.386	0.417	0.615	0.411
Ca	0.007	0.048	0.538	0.573	0.554	0.044	0.363	0.322	0.311	0.207	0.299
Na	0.053	0.280	0.087	0.145	0.548	0.777	0.157	0.211	0.148	0.139	0.177
K	0.008	0.040	0.012	0.012	0.100	0.214	0.059	0.059	0.050	0.030	0.045
Ti	0.000	0.000	0.011	0.012	0.010	0.008	0.023	0.024	0.016	0.016	0.023
Octahedral	2.186	2.300	1.532	1.530	2.093	1.955	1.765	1.761	1.667	1.707	1.699
6 (O)	Clinopyroxene structure										
Si	1.384	1.386	1.847	1.860	1.570	1.568	1.628	1.645	1.699	1.646	1.675
Al4+	0.000	0.027	0.130	0.140	0.430	0.432	0.372	0.355	0.301	0.354	0.325
Ti4+	0.000	0.005	0.017	0.000	0.000	0.000	0.000	0.000	0.000	0.000	0.000
Fe3+	0.616	0.582	0.006	0.000	0.000	0.000	0.000	0.000	0.000	0.000	0.000
Ti6+	0.000	0.000	0.000	0.018	0.015	0.012	0.034	0.036	0.024	0.025	0.034
Al6+	0.000	0.000	0.000	0.028	0.030	0.894	0.077	0.116	0.151	0.148	0.141
Fe	0.210	0.211	0.197	0.256	0.192	0.013	0.709	0.666	0.636	0.546	0.651
Mg	2.350	2.075	0.991	0.759	0.743	0.030	0.586	0.579	0.625	0.922	0.616
Ca	0.010	0.071	0.808	0.859	0.831	0.066	0.545	0.484	0.467	0.311	0.449
Na	0.079	0.420	0.131	0.217	0.822	1.165	0.236	0.316	0.222	0.209	0.265
K	0.013	0.060	0.018	0.018	0.150	0.321	0.088	0.088	0.076	0.046	0.067
Octahedral	2.662	2.838	2.144	2.156	2.783	2.500	2.275	2.286	2.200	2.206	2.224
mg	74.0	72.3	83.0	74.8	79.4	69.3	45.2	46.5	49.5	62.8	48.6
Cr ppm	300	800	1700	900	1200	1200	1100	1400	500	2600	500
Ni	1200	1700	2100	2000	2200	1900	2500	3100	2500	3900	2400
Ce	0	1300	2200	1900	3400	2800	5700	4000	1700	5400	1800
Ba	1400	0	800	3300	1200	0	0	1400	2800	0	0
Sr	3000	4800	4700	8000	3700	6500	12400	8500	0	0	13800
S	900	1600	1200	1200	3700	700	1900	1300	700	1100	0
Fo	71.44	58.69	14.04	5.09	2.64	0.00	12.98	13.60	15.88	28.67	15.82
Mont	0.47	2.99	58.78	56.46	42.26	3.10	18.85	17.28	18.67	15.39	17.34
Kir	0.16	1.14	12.07	19.03	10.94	1.37	22.84	19.86	19.02	9.12	18.35
Fa	25.13	22.44	2.88	1.71	0.68	0.00	15.73	15.63	16.18	16.99	16.74
NaKAl ol	2.80	14.74	12.22	17.71	43.47	95.53	29.59	33.63	30.25	29.84	31.75
ol saturated	1828	1267	745	568	468	21	674	639	658	846	667
qz saturated	–39	67	42	30	–529	–1156	–231	–263	–141	–140	–182
wo	0	0	0	0	0	20	0	0	0	0	0
Diop	13	84	1198	1135	1109	56	410	378	394	341	370
en	1944	1648	286	102	69	0	283	298	335	635	338
Hed	4	32	246	382	287	24	497	435	402	202	392
fs	684	630	59	34	18	0	343	342	342	376	358
Jd	0	44	233	297	646	2411	540	680	507	445	565
Ac	152	740	33	118	988	293	0	0	0	0	0
wo + di + en	70	54	72	60	38	3	33	32	37	49	35
jd + ac	5	25	13	20	52	96	26	32	26	22	28
hed + fs	25	21	15	20	10	1	41	36	38	29	37
q	–824	–1024	–202	–214	–899	–689	–358	–375	–266	–281	–300
cpx	2798	3178	2055	2069	3117	2803	2072	2132	1980	1999	2023

wo + di + en, Wollatonite + diopside + enstatite; jd + ac, Jadeite + acmite; hed + fs, Hedenbergite + ferrosilite.

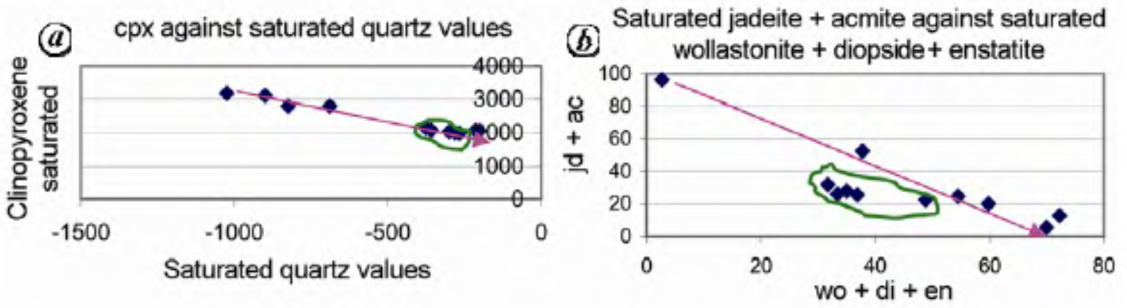

Figure 2. ***a***, The analyses are deficient in quartz values to form saturated clinopyroxene (cpx) cations. cpx from ultrabasic rock (ubr) falls in a separate field. The cpx from shon shows wide compositional variations indicating that the grain was subjected to prolonged period of magmatic growth under liquid condition. Trend of magmatic evolution of cpx in ubr. ***b***, Magmatic evolution of cpx components.

site. The structural formulae (Table 1) for cpx calculated on the basis of 6(O) show that Mg and Fe^{iii+} ions decrease during the course of magmatic evolution in shon and Ca ions decrease steadily in cpx from ubr. Other ions show oscillatory variations during the course of magmatic evolution. Figure 2 shows a common magmatic crystallization trend for both shon and ubr. The analyses for ol grain in shon show wide compositional variation indicating its crystallization under liquid condition for a prolonged period during magmatic evolution[3]. The small field of chemical variation in the grain from ubr indicates its rapid intermediate crystallization and fractionation of the ol grain. All the analyses show significant enrichment of calcium, alkalis and aluminum. The extreme amounts of calcium, alkalis and alumina in the ol grain analyses favour the calculation of cpx members such as wollastonite, enstatite, ferrsilite, diopside, hedenbergite, jadeite and aegirine. Normative proportions of cpx components of wollastonite–diopside–enstatite, ferrosilite–hedenbergite and jadeite–acmite were calculated and their percentages plotted to trace the trend of magmatic evolution (Figure 2 *b*). The figure indicates that the ol grain is subjected to extensive transformation along its peripheral portion. This feature is further explained in Figure 3 *a–f*.

Trace elements distribution of Cr–Ni, Ce and S plotted against the mg number (100*Mg/(Mg + Fe)) shows parallel trends of magmatic evolution for the analyses carried out for both ol grains in these two different rocks. The high Cr–Ni ppm variations with their corresponding low mg number indicate separate fields for the analyses carried out for the ol grain in ubr. On the other hand, the analyses carried out for the ol grain in shon show the same trend of wide variation, but along a linear magmatic trend (Figure 3 *a–c*). The distribution of saturated hypersthene and enstatite against negative values of *q* shows similar pattern of trends, but the trend is limited for the analyses of the grain in ubr (Figure 3 *d*). This pattern further supports the distribution of saturated ol components against *q* values for the two ol grains (Figure 3 *e*). The distribution of normative proportions of monticellite against NaKAl-orthosilicates further confirms the linear evolution of magmatic crystallization (Figure 3 *f*).

Figure 3 *g* represents compositional variations of ol components. The general direction of magmatic trends for saturated ol components against quartz values shows that the trend for forsterite and fayalite components decreases during magmatic evolution; monticellite and kirschsteynite components steadily increase and the trend for NaKAl-orthosilicate is slightly decreasing, indicating that the original magma is enriched with significant amount of alkali constituents. The alkali-lime index[7] on silica for these olivinites falls at 37.5%, indicating that they belong to the alkali suite of rocks (Figure 3 *h*).

The high degree of oxidation ($Ox° = 100*Fe^{iii+}/(Fe^{iii+} + Fe^{ii+}Mn^{ii+})$) of bulk rock composition of shon[3] around 60 indicates that the rock is composed of significant amount of ferric iron leading to the formation of aegirine consuming required alkalis. Before the crystallization of calcic-plagioclase, the peripheral portions of the early fractionated ol reacted with the residual magma and its peripheral portion transformed into diopside on slow cooling with increasing magmatic pressure by incorporating CaO. The early crystallization of diopside at the expense of ol components, the residual magma is under-saturated with silica. Significant enrichment of CaO in the magma is a pre-requisite for the enrichment of sodium in the ol structure[8]. Under increasing pressure more Al_2O_3 is incorporated into the diopside. Further increasing Na_2O with available ferric iron peripheral growth of aegirine-augite and aegirine develops. In the absence of crystallization of plagioclase in shon, with increasing constituents of Na_2O and Al_2O_3 and impoverishment of SiO_2 and Fe_2O_3, jadeite crystallizes from the residual magma along the peripheral portion of ol or cpx[9,10]. Such crystallization of jadeite[9,10] takes place at the expense of peripheral ol components in the temperature range 600°–800° with pressure ranging from 10 to 20 kbar. Very high enrichments of Al and Na with progressive decrease in silica activity indicate substitutions of Mg, Si ↔ Al, Al; Mg, Ca ↔ Al, Na transforming peripheral ol or cpx into alumina rich jadeite.

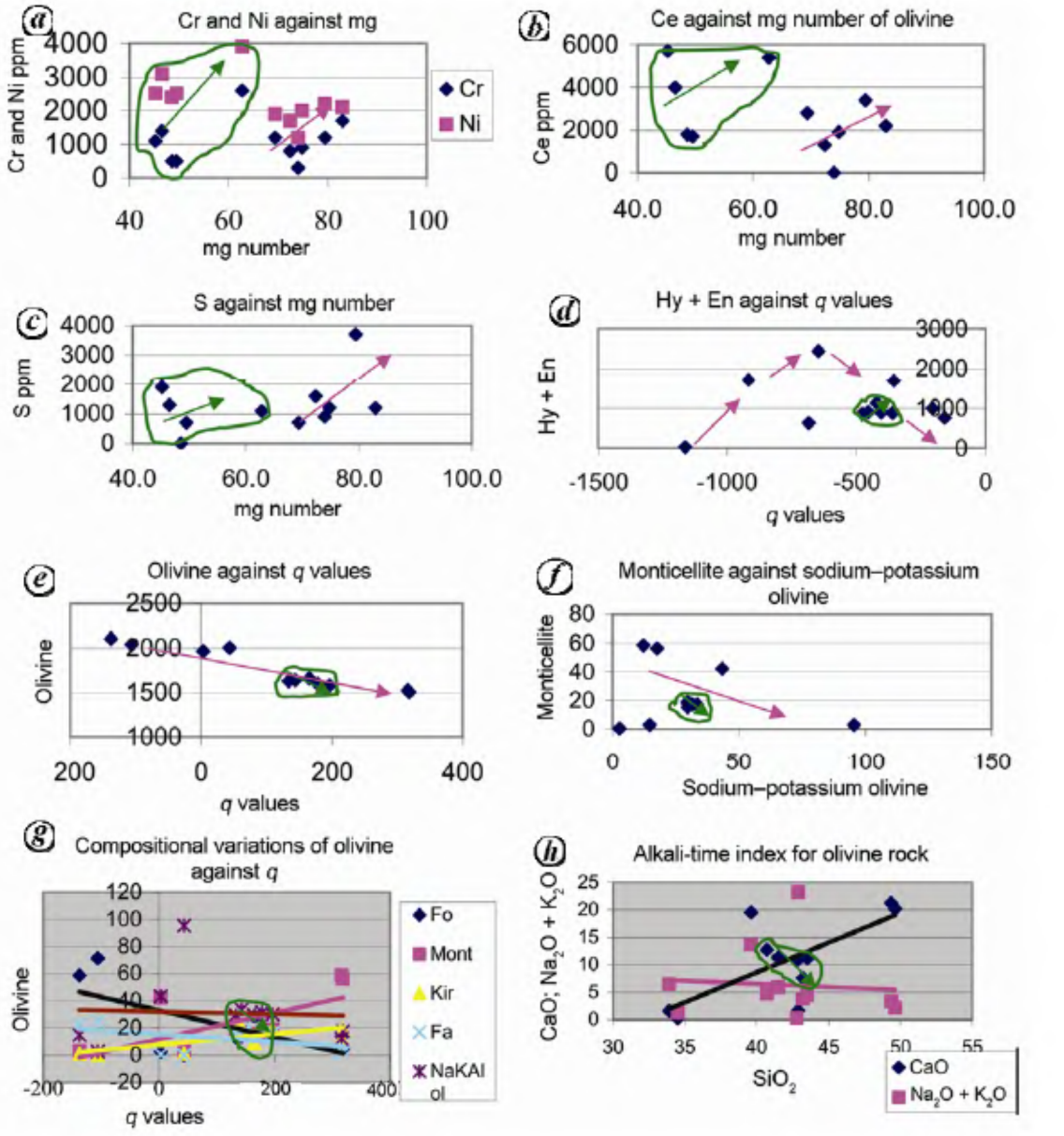

Figure 3. ***a–c***, Separate linear magmatic trends for the distribution of Cr–Ni, Ce and S respectively, against their mg numbers. ***d***, Saturated normative proportions of Hy + En and against their q values show wide compositional linear variations for the olivine grain in shon and a limited variations for the olivine grain in ultrabasic rock. ***e***, Similar trends are also supportive of the distribution of saturated olivine normative proportions and their q values. ***f***, Distribution of normative proportions of monticellite against sodium–potassium orthosilicates further confirms the similar trends of magmatic evolution. ***g***, Linear distribution of normative proportions of olivine components shows their magmatic evolution. ***h***, Alkali-lime index = SiO_2 content (37.5%) at which CaO% equals ($Na_2O + K_2O$)% at which CaO equals ($Na_2O + K_2O$). This feature indicates that they belong to alkali suite of igneous rocks.

The formation of jadeite compensates the silica deficiency by avoiding the crystallization of nepheline and albite[11].

$$2\text{Jadeite } (NaAl_2Si_2O_6) \leftrightarrow \text{Nepheline } (NaAlSiO_4) + \text{Albite } (NaAlSi_3O_8).$$

The crystallization of jadeite consuming Na_2O and Al_2O_3 obliterates the crystallization of albite and nepheline in the residual magma and crystallization of potassium feldspar takes place consuming residual K_2O, Al_2O_3 and SiO_2 from the magma[11]. Thus, development of jadeite produces silica under saturated nepheline-free shon rocks with crystallization of potassium feldspars from the residual magma as end-products. With increasing vapour pressure during late magmatic processes, particularly under high P_{CO_2} pressure, the mafic cumulates are unstable and release more Ca to the melt. The Ca-enriched residual

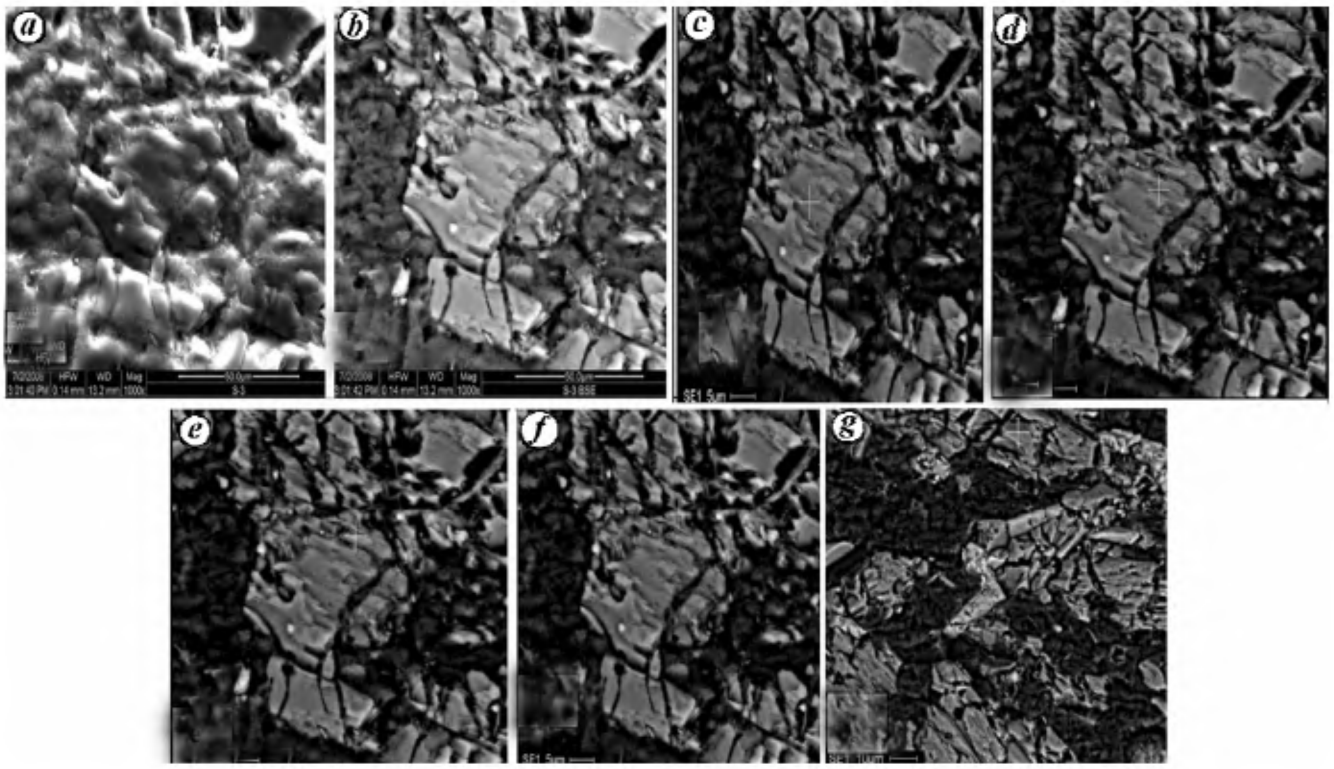

Figure 4. Back scattered image of olivine grains in ubr. ***a***, Electron microscopic image of the ultrabasic rock × 1000. ***b***, Back scattered image of olivine grain × 1000. ***c–f***, points for which analyses 1 to 4 are made from an olivine grain core to periphery. ***g***, point for which analysis 5 is made from a discrete olivine grain.

magma immiscibly separates into silicate and carbonate magmas under high P_{CO_2}. Further differentiation of these magmas produces a series of alkali syenites and carbonatites successively emplaced in a sequential order at first in the Sevvattur basin and then in the Jogipatti basin, resulting in the formation of a zoned alkali carbonatite complex of Tiruppattur, Tamil Nadu[3].

1. Ramasamy, R., Geology of the area SW of Tiruppattur, North Arcot District, Madras State (Tamil Nadu), Ph D thesis, University of Madras, Chennai, 1993.
2. Ramasamy, R., Structure and tectonics of carbonatite complex of Tiruppattur, Tamil Nadu. Current Trends in Geology. *Proc. IV Indian Geology Congress*, Today and Tomorrow's Printers and Publishers, New Delhi, 1982, vol. 7, pp. 119–136.
3. Saravanan, S. and Ramasamy, R., Geochemistry and petrogenesis of *Shon* and associated alkaline rocks of Tiruppattur carbonatite complex, Tamil Nadu. *J. Geol. Soc. India*, 1995, **46**, 235–243.
4. Ramasamy, R., Ca-rich pyroxenes from the carbonatite complex of Tiruppattur, Tamil Nadu. *Curr. Sci.*, 1986, **55**, 981–984.
5. Rittmann, A., *Stable Mineral Assemblages of Igneous Rocks*, Springer-Verlag, Berlin, 1973, p. 262.
6. Kampata, D. M., Nixon, P. H. and Salemink, J., Monticellite in Gwena Kimberlite (Shaba, Zaire): Evidence of late magmatic crystallization. *Mineral. Mag.*, 1994, **58**, 496–501.
7. Peacock, M. A., Classification of igneous rock series. *J. Geol.*, 1931, **39**, 54–67.
8. Fodor, R. V., Keil, K. and Bunc, T. E., Contributions to the mineral chemistry of Hawaaiian rocks, IV. Olivines in rocks from Haleakala and West Maui volcanoes. *Pac. Sci.*, 1977, **31**.
9. Deer, W. A., Howie, R. A. and Zussman, J., *An Introduction to the Rock Forming Minerals*, Prentice Hall, London, 1992, p. 695.
10. Butvina, V. and Livin, Y., Physico-chemical transition from peridotite assemblage to the eclogite one (experimental data at 7.0 GPa), *Geophys. Res. Abstr.*, 2010, **12**, EGU2010-3717-1.
11. Yagi, K., Petrochemical studies on the alkalic rocks of the Morotu District, Sakhalin, *GSA Bull.*, 1953, **64**, 769–810.

ACKNOWLEDGEMENTS. We thank Dr P. Shanmugam, Department of Ocean Engineering, IITM, Chennai and V. Subramanya Sarma and S. Santhi, Metallurgical Laboratory, IITM for carrying out electron microprobe analyses.

Received 13 July 2009; revised accepted 21 September 2010